HUMAN KINEMATICS DURING NON-COLLINEAR LOW VELOCITY REAR END COLLISIONS

Whitman E. McConnell, Herbert M. Guzman, Scott W. Krenrich, John B. Bomar, Jr., Richard M. Harding, James H. Raddin, Jr., and **James R. Funk**
Biodynamic Research Corporation
San Antonio Texas, USA

Darrin A. Smith
Injury Sciences LLC
San Antonio, Texas, USA

ABSTRACT

Non-collinear low velocity rear end (LVRE) collision human kinematics have not previously been studied. Occupant head and neck motions during twenty similar non-collinear (15 and 30 degree angle) left rear end collisions were analyzed for five male test subjects alternately positioned in the left and right front seats of the struck vehicle. Displacement-time and acceleration data for occupant, seat, and vehicles were determined by 3D motion analyses and linear accelerometer outputs. The dynamics of the struck vehicle at 6.0 to 9.3 kph (3.8 to 5.8 mph) delta-V showed an initial period of yaw, even when the rear tires did not lose traction with the pavement. The brief yaw seen during the 15 degree impacts was accompanied by early relative rightward movement of the vehicle's seat and seatback behind the stationary test subject: the subjects subsequently engaged the left region of the seatback and head restraint. A more pronounced yaw accompanied the loss of rear tire traction during the 30 degree tests, and resulted in occupant contact/loading further toward the left edge of the seat back and head restraint. For a given striking vehicle velocity, the impact severity in terms of head acceleration and changes in head velocity were significantly lower ($p<0.05$) at vehicle impact angles of 30 degrees compared with 15 degrees. Clinically, there were only minor short-term symptoms and no long-term symptoms observed in these angled impacts.

Low velocity rear end (LVRE) human testing has been previously reported by a number of investigators over a range of velocity change, and with a wide population of subjects, including females. Other variables, frequently found in “real world” vehicle collisions, have not been well explored, and we have been unable to find any published studies of the human kinematics of non-collinear (angled) LVRE collisions over the last ten years.

These events happen during intersection and parking lot impacts that can occur, for example, when the leading (angled) vehicle turns onto an intersecting lane, unexpectedly slows or stops, and is struck from behind by the following vehicle (Fig. 1).

Fig. 1 - Staged Non-Collinear LVRE Collision

A principal aim of this study was to explore the hypothesis that angled non-collinear LVRE collisions would impose a different pattern of accelerations upon an occupant, and produce head and neck kinematics out of the sagittal plane, when compared to those seen during collinear LVRE collisions.

This paper reports the test subject and vehicle data obtained from high speed film based (HSF-based) time-displacement measurements and accelerometer outputs, and the analysis of the vehicle dynamics and the kinematic responses of each subject for four test conditions. Potential similarities and differences in the kinematic responses recorded for each subject in the four test positions and then among the five subjects for each position were defined, compared and summarized.

METHODS

In order to study occupant kinematics during non-collinear impact conditions, an angled LVRE collision testing protocol was developed using the Biodynamic Research Corporation’s (BRC) Research Test Center (RTC) indoor low velocity collision test facilities, linear accelerometers, angular rate sensors, recent advances in precision 3-dimensional motion analysis, and its existing research subject pool. This study was conducted with a five volunteer subject panel, each of whom participated in four tests using a matrix of two seat positions and two impact scenarios (Table 1).

Table 1 - Test Matrix

		Seat Position	
		Driver	**Right Front**
Impact angle (leftward)	15º	n = 5	n = 5
	30º	n = 5	n = 5

VEHICLES AND TEST SITE - Two specially prepared vehicles were used for all twenty tests. One vehicle (an unmanned 1996 Buick Skylark) was used as the striking vehicle and the other vehicle (a 1996 Ford Taurus) was the struck vehicle, occupied by the test subjects. Both vehicles were equipped with automated electro-pneumatic brake pedal operators. The front seats of the Ford were of typical American sedan "bucket" style, with the seat back recliner and locking mechanism on the outboard side. The same seats and same fore-aft and seat back angle positions were used throughout testing. Several modifications were made to the test-vehicles for practical and safety reasons. Steering was fixed in a straight ahead neutral position for both, and no vehicle control action was required of the subject during testing. Foam rectangles were placed behind the occupied front seat to safeguard against excessive deformation of the seatback, and the driver's door was removed to allow for photographic access. For each test, the factory standard head restraints (approximately 28 cm (11 in) wide)) in the target vehicle were kept in their fully raised position, as were the B-pillar D-rings of the standard 3-point adjustable restraint systems. Standard 205/65R15 tires with minimal tread wear on the struck vehicle were kept at factory recommended tire pressures throughout the study. Each vehicle was inspected before and after each test run for safety or functional problems. Vehicle repairs and minor parts replacement, including that of various bumper system components, were made as necessary on both.

Fig. 2 - Test Area and Vehicle Orientation

The indoor test area is housed in a warehouse building with a large doorway leading to an indoor-outdoor steel ramp allowing up to a 2.4 m (8 ft) elevation above the test area floor (Fig. 2).

The 12 degree incline provides a method of controlling the striking vehicle's energy. A 9.1 m (30 ft) roll out zone prior to the impact point allowed vertical perturbations of the striking vehicle to cease before impact. By using the same starting position on the ramp for each test, similar impact velocities were achieved (all within 12.0 ± 0.4 kph (7.45 ± 0.25 mph). The car to ground coefficient of friction of the struck Ford was measured by dragging the vehicle over the test area floor.

TEST SUBJECTS - The protocol for this study was reviewed by the University of Texas Health Science Center (UTHSC) Institutional Review Board (IRB), and the use of human test subjects selected from the staff of BRC was approved by UTHSC IRB Protocol #901-0099-006, under DHHS Regulation 46.110(3). The age, height, and weight of each of the five fully informed, healthy, volunteer male test subjects is provided at Table 2.

Table 2 - Test Subject Data

Test Subject	**Age** (start of testing)	**Height** cm (in)	**Weight** kg (lb)
01	60	176.5 (69.5)	95.3 (210)
02	48	180.3 (71.0)	81.6 (180)
03	49	175.3 (69.0)	79.4 (175)
04	49	188.0 (74.0)	99.8 (220)
05	55	180.3 (71.0)	106.6 (235)

Prior to testing each subject completed a general medical history form with intent to discover any underlying medical or surgical problems. This history was reviewed by the examining physician in the presence of the test subject. Any questions suggested by the form data or discovered during the general physician's interview were explored and noted. Each subject then underwent a physical evaluation tailored after the "hands on" portion of a standard USAF flight physical examination. Also included were radiographic imaging studies of their cervical spines and measurements of voluntary maximum neck

Fig. 3 - Test Subject Marking

range of motion and normal sitting head carriage angles. No disqualifying defects, based on the requirements set out by USAF flying Class III physical standards, were found. Subject marking (Fig. 3) for later photographic analysis was by means of adhesive targets placed on an individually fitted bite block and accelerometer assembly; on a lightweight adjustable headband; and at locations over the mastoid prominence (as an approximation of the lateral projection of the upper end of the cervical spine), over both maxillary prominences, over the spinous prominence of the seventh cervical vertebra, and over the manubrial notch. Targets were also placed on the subject's clothing over the left shoulder and lateral upper thigh/hip to provide non-fixed approximations to track these areas. Test runs for each subject were intended to take place at least one week apart to avoid any cumulative effect from multiple test exposures within a short time period. Subjects were asked to assume a normal seated posture (drivers placed both hands normally on the wheel) and to be as relaxed as possible. Test subjects were interviewed for any interval medical history by a physician before and after each test run, physical examinations conducted when there was a change noted and follow-up inquiries made at periodic intervals following the testing. There were no physical findings arising from this study. All findings, which were limited to subjective symptoms only in this study, were reported in the Appendix A summary information section.

ELECTRONIC DATA ACQUISITION - For all tests, the subjects were instrumented with bite blocks (Fig. 4) rigidly located with respect to the skull. Three mutually orthogonal linear accelerometers were mounted on each bite block to measure fore-aft (Gx), lateral (Gy), and vertical (Gz) acceleration. The block also housed two rate sensors to measure head pitch (ωy) and yaw (ωz) angular velocities (i.e. in the sagittal and transverse planes, respectively).

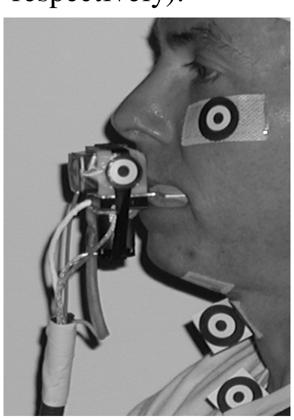

Fig. 4 – Transducer & Marks

Accelerometers measuring linear Gx, Gy, and Gz acceleration were mounted near the centers of gravity (CG) of both test vehicles, and the struck vehicle was also instrumented with an angular rate sensor to measure its yaw (ωz) velocity.

The closing velocity of the striking vehicle was determined using a speed trap which consisted of a succession of tape switch contacts. Two infra-red (IR) sensors mounted near the CG of the struck vehicle were aimed through an opening in the floor-pan to detect a succession of reflective strip targets on the floor, and so provide a time-history of the displacement of the vehicle in the fore-aft (x) and lateral (y) directions, and hence its resultant change in velocity (Delta-V). This measurement system was used to cross check the calculated velocity of the struck vehicle at its CG with accelerometer and HSF data. Synchronization of film and transducer data was achieved by electronic strobe light in the field of view of the HSF cameras and by electronic recording when the bumper tape switches were triggered. The signals from all sensors (i.e. bite block and vehicle accelerometers, angular rate sensors, and speed traps) were sampled at 10,000 Hz. The accelerometer and rate sensor data were then filtered with a CFC 1000 (1,650 Hz upper cut-off) analog filter in accordance with SAE J-211. The data acquisition system was triggered manually prior to release of the striking vehicle and ceased automatically several seconds after both vehicles came to a stop.

HSF DATA ACQUISITION - Detailed high speed photographic documentation of the test runs was performed in accordance with SAE J-211/2 recommended practices, and accomplished with two 16-mm high-speed cameras running at 500 frames per second. During each test run, the cameras were placed at two fixed positions approximately 9.1 - 12.2 m (30 - 40 ft) from the front and left side of the struck vehicle and arranged to record the first 1.83 – 2.44 m (6 - 8 ft) of the occupant's horizontal movement. After each test run, a specially constructed three dimensional rectangular open box calibrator (Fig. 5) was placed within the test area field of view and photographed by three stationary HSF cameras on the same film that contained the subject test run exposures. The calibration process enabled a commercial software application to track the points of interest within the overlapped view of the two cameras, in three dimensions, in 2 msec increments.

Additionally, for a number of the 15 and 30 degree tests, a chalk/water based mixture was painted on the outside tread of all four tires of the struck vehicle to record the track and trajectory of the front and rear wheels. These floor tracks were measured and photographed after each such test.

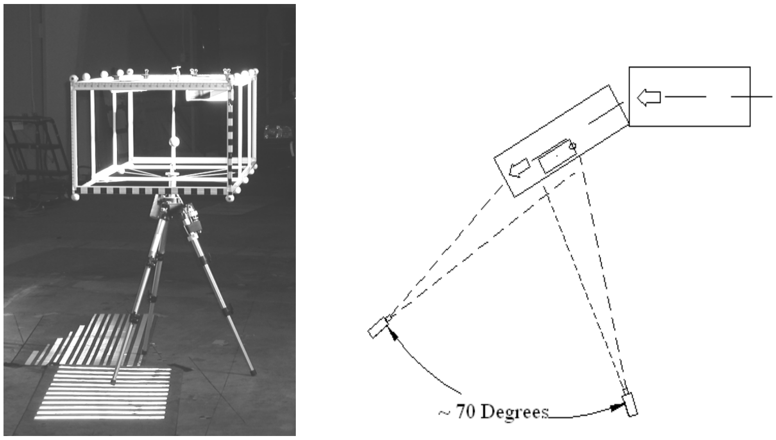

Fig. 5 - Calibrator Image and Set Up Diagram

LINE OF ACTION - To define and standardize the two angled test collision scenarios, the vehicle positions at contact were characterized by the angle and position of the striking vehicle's line of action (the trajectory pathway of the striking vehicle's CG) with respect to the struck vehicle's CG (Fig. 6).

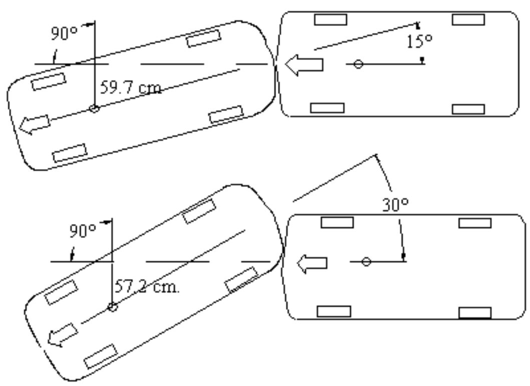

Fig. 6 – Test Configuration: 15 & 30 degrees

For these tests, the line of action for the 15 and 30 degree series was 59.7 cm (23.5 in) and 57.2 cm (22.5 in) rightward of the struck vehicle's CG respectively. The Ford's rounded rear bumper and shape of the Buick's front bumper prevented any further reduction of the distance from the struck vehicle's CG and striking vehicle's line of action.

TEST PROCEDURES - For each test the striking vehicle was backed up the ramp to the same starting position and held by a quick release mechanism and safety chocks. The struck vehicle was then precisely aligned at the impact point by using floor markings for either the 15 or 30 degree leftward impact angle positions. After a safety check, the ramp chocks were removed, the lights turned on, and data recording started as the striking vehicle was released to roll down the ramp to the impact point. Prior to impact, the three HSF cameras were started. Complete masking of the impending impact from the test subjects was impractical. However the time of impact was varied so that the test subjects could not closely predict impact within about a 40-60 second period of time. Our unpublished testing has indicated no difference in test subject kinematic responses, whether fully aware of the precise impact time or not. After every test collision, the subject's physical condition and symptom experience was checked and recorded, a post test assessment of vehicle damage was completed, and electronic-photographic test data storage was confirmed.

PROCESSING OF SENSOR DATA - The power spectral density for each of the accelerometer signals was obtained in order to analyze its frequency content, and to verify that, if necessary, filtering with a lower cut-off frequency could be performed. It was determined that all accelerometer signals could be filtered with a CFC-180 (300 Hz upper cut-off) or higher cut-off filter. Subsequently, vehicle accelerations were filtered with a CFC-180 filter and compared with the original signals (filtered with CFC 1000) to confirm that additional filtering would not significantly attenuate them. The angular rates recorded from the bite block sensors were similarly filtered and differentiated to obtain angular accelerations.

PROCESSING AND ANALYSIS OF FILM DATA - The frame accurate .avi files derived from the HSF for each of the 20 test runs were input to the computer for analysis. For this study, the targets tracked were the middle of the head (estimated CG), the left mastoid prominence, the junction of C7 and T1, the bite block, and a point estimated to be at the subject’s sacrum. A target was placed on the upper mid-windshield of the struck vehicle, to represent the vertical extension of the vehicle’s CG, and at a point at the mid-base of the windshield. Both marks were tracked to determine the vehicle’s velocity and angular motion over time. Additionally, two immobile points were selected to provide an earth-based reference for the motion data.

VALIDATION OF MOTION ANALYSIS RESULTS – Because of the angular and translational motion of the bite block accelerometers, transforming these signals to the head CG’s reference frame was mathematically complex and nonlinear. The 3-D motion analysis package appeared to greatly simplify this process, but extensive validation was undertaken. The validation included off-angle collisions with a Hybrid III 50th %-ile ATD instrumented with dual accelerometer arrays at a simulated bite block and inside the ATD's skull at the head's CG. There was a close correlation between all data recorded by both [film and sensor] methods in the range of accelerations that are biomechanically relevant. The digitized (film) occupant and vehicle displacement-time data were recorded at a nominal 500 frames per second, and their power spectral densities obtained to analyze their frequency content. It was determined that the film displacement-time data could be low-pass filtered with an upper cut-off of 20 Hz. The film data were then differentiated and the resulting velocities and accelerations compared with the accelerometer and integrated accelerometer results (Fig. 7).

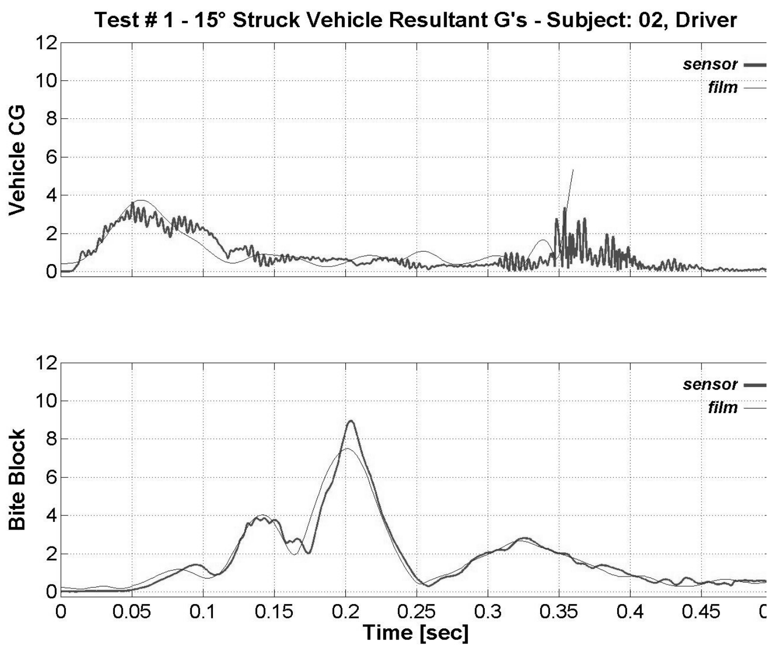

Fig. 7 – Comparison of Motion Analysis and Sensor Data

Tracking between the film-derived accelerations and the accelerometer data had correlations of 96-99%, and an average deviation of 8.8%. Furthermore, based on cross-correlation in time between the two data sources, the average time shift was 3.3 msec.

STATISTICAL EVALUATION - For this study, two vehicle targets and four subject targets were tracked and analyzed for all tests. The raw digitized displacement data for each target were recorded and mathematically treated to produce resultant acceleration *vs.* time data. The Matched-Pair Wilcoxon Signed-Ranks Test was employed to assess the peak head resultant acceleration and peak velocity change differences for the driver and passenger seating positions at each angled condition. Two estimates of head resultant acceleration were used: head CG acceleration (from digitized film), and the bite-block acceleration. Each subject served as his own control. Because of the small sample size, exact tables for the Wilcoxon analysis were used to assess the significance of the calculated rank sums.

RESULTS

VEHICLE DYNAMICS - In this study, the appearance of a yaw component in response to the angled impacts complicated the analysis both of the vehicle and the occupant. Conventional high energy (higher velocity change) reconstruction techniques generally discount tire friction forces because they are relatively small when compared to the much higher collision forces. This is not true for non-collinear low velocity collisions where, because of the yaw induced on the struck vehicle in such events, each point of the struck
vehicle has a different velocity change until yaw and acceleration cease.

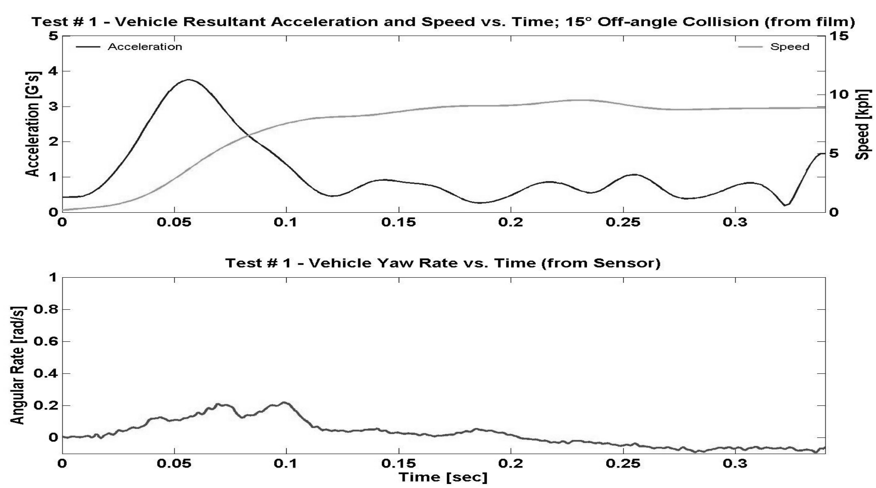

Fig. 8 - 15^0 Impact: Struck Vehicle Resultant Acceleration/Velocity Change

LVRE COLLISION DYNAMICS AT 15 DEGREES - The rear tires of the struck vehicle in all 15 degree tests did not move laterally as the vehicle moved forward. Fig. 8 shows a typical struck vehicle velocity change and acceleration profile for a 15 degree test. The velocity change imparted to the struck vehicle stayed consistent throughout the study.

The rear of the car did move rightward with respect to the tire's ground contact area as the cross section of the rear tires rolled in that direction, and the suspension system was seen to "heave" rightward and upward during the early impact period, but the final vehicle trajectory did not change from its original 15 degree heading. Observation of the films, however, revealed that there was enough lateral motion to change occupant loading on the seatbacks in a leftward as well as a rearward direction.

LVRE COLLISION DYNAMICS AT 30 DEGREES - The rear tires in this series of collisions were unable to maintain lateral traction and underwent lateral sideslip (range 25 - 56 cm (10 - 22 in)) as the vehicle moved forward. The (fixed) neutral angle front tires did not sideslip, but the chalk tracks indicated that the whole vehicle was rotating around a point located near the left front tire. This point varied during the 30 degree tests from several inches inboard of the left front tire to six or more inches outboard of its tread. Fig. 9 shows the velocity change and acceleration profile for the struck vehicle in a typical 30 degree test.

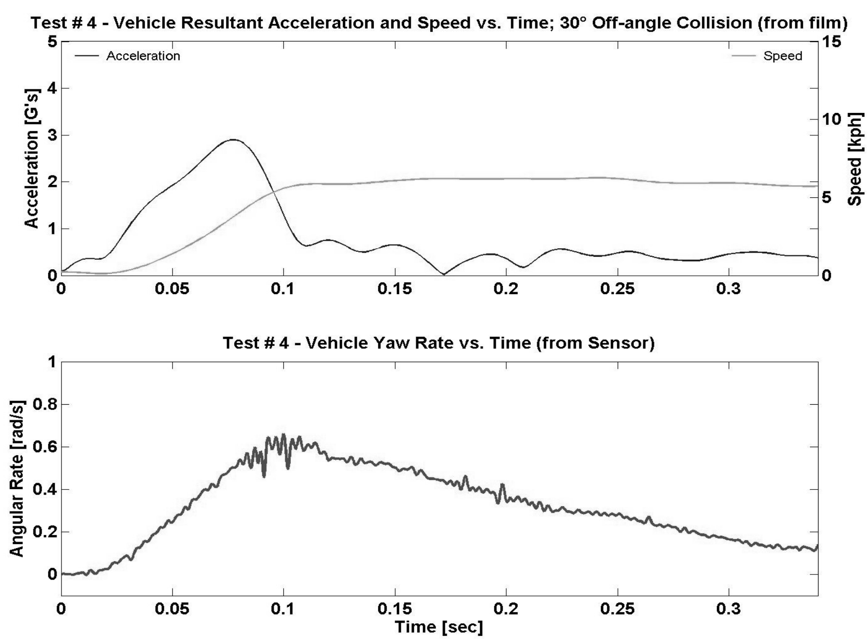

Fig. 9 – 30^{0} struck Vehicle Resultant Acceleration/Velocity Change

In comparison to the 15 degree tests, increasing the impact angle while maintaining the same input energy resulted in a decrease in overall velocity change of the struck vehicle and also altered the crash pulse shape and duration. During impact, the rear end of the struck Ford slewed rightward; scrubbing the rear tire treads across the pavement and thus the final velocity change was lower. Fig. 10 shows the right rear tire mark from a 30 degree test.

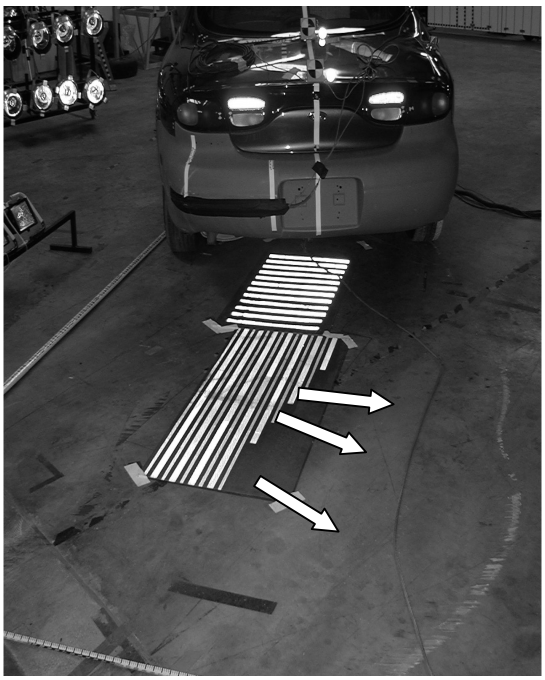

Fig. 10 - 30 degree impact: Right Rear Tire Track (Arrows)

Average yaw was 10 to 20 degrees for the 30 degree test series. Fig. 11 is a diagram of a vehicle yawing about a point, and of the resulting occupant loading directions for different seat positions.

From inspection of the motion of the struck vehicle shown in this Fig., points on the vehicle further away from the center of rotation will experience a greater velocity change during the yaw.

With regard to the integrity of the test vehicles throughout the study: there was a gradual crushing of the front bumper support structures of the Buick, but no identifiable change in the collision performance (Delta-V and acceleration profiles) of the Ford; restraint system function was normal and did not change throughout the testing period; no changes in mechanical seat characteristics were observed and their structure was undamaged; the safety foam did not influence seat performance or occupant kinematics; and there was no impact-related deformation of the Ford's door opening. In addition, the coefficient of friction of the tire/floor interface remained at 0.6 throughout.

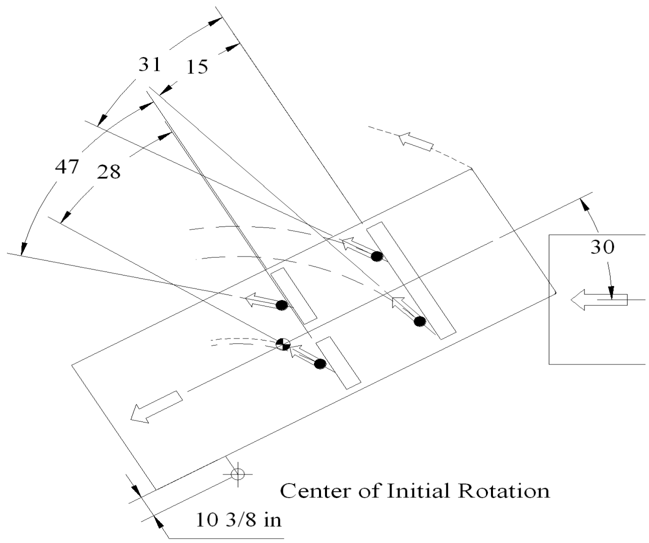

Fig. 11 -Variations of Force Direction in Degrees by Seat Position

OCCUPANT KINEMATICS - Details of the occupant kinematics associated with collinear LVRE collisions have been described many times. This test series demonstrated that the kinematics observed in non-collinear test events is fundamentally similar. Thus, although, even in the 15 degree tests, the impact related vehicle yaw modified the occupants' responses and, to some degree, the onset rate and shape of the observed acceleration pulse and duration, in no case did the maximum extent of impact related head and neck motion meet or exceed the measured range of the individual subject's normal voluntary head and neck motion.

The following is a descriptive account (based on McConnell's earlier approach [McConnell et al, 1993, 1995]) focusing primarily on the principal observed differences between collinear LVRE collision kinematics and the observed occupant kinematics for the 15 and 30 degree non-collinear LVRE test collisions (Fig. 12).

Phase 1 - Initial Response (0-100 msec) – The 30 degree tests showed more rightward seat back movement than the 15 degree tests, which resulted in increased subject loading of the left side of the seat back, and the center of the upper torso loading area moved further leftward. In the 15 degree tests, the head restraint yawed and moved forward to intercept the center line of the head about half way between its center and its left edge. During the 30 degree tests, the head centerline intersected the head restraint near its left edge (Figs. 12a, b).

Phase 2 - Principal Forward Acceleration (100-200 msec) - In the 15 degree tests, a counterclockwise yaw (< 5 degrees lateral rotation) of the subject's head occurred as it fully engaged the head restraint. In the 30 degree tests, there was a larger counterclockwise yaw and left lateral neck flexion, as the occipital surface of the head rolled around the left edge of the head restraint (Figs. 12c, d).

Figs 12 a - h Subject 01 in the passenger seat at synchronized times during the 15 and 30 degree test runs.

Fig. 12a - 15 degree test at 100 msec

Fig. 12b - 30 degree test at 100 msec

Fig. 12c - 15 degree test at 200 msec

Fig. 12d - 30 degree test at 200 msec

Fig. 12e - 15 degree test at 300 msec

Fig. 12f - 30 degree test at 300 msec

Fig 12g – 15 degree test at 400 msec

Fig 12h – 30 degree test at 400 msec

Phase 3 - Head Over speed and Torso Recovery (200-300 msec) - The head and torso, having loaded the left side of the seat back as the seat back was moving relatively rightward, departed in a forward and rightward direction relative to the new seat/seat back orientation. For the 15 degree tests this angle was slight, but noticeable. The 30 degree test departure angle was obvious. By about 250-320 msec, the head was starting to approach the 12:00 o'clock position, and for the 15 degree tests, it was then aligned perpendicularly with the shoulders. The 30 degree tests required longer to align the head and shoulders (Figs. 12e, f).

Phase 4 - Head Deceleration/Torso Rest (300-400 msec) and Phase 5 – Restitution (400-600 msec) – During this phase there was some lateral torso/head rocking back and forth (more noticeable in the 30 degree than in the 15 degree tests), as the subject's restitution progressed to completion (Figs. 12g, h).

HEAD CONTACT - The possibility of slight head contact with the left upper B-pillar and door header area was predicted, and indeed there was light head impact of a very low magnitude (HIC < 3) during four of the five driver side tests at 30 degrees. The head contacts produced no physical findings or symptoms, and were perceived as very mild.

QUANTIFICATION OF OCCUPANT MOTION – Figs. 13- 16 are combined graphic representations of the head accelerations for all subjects and for each of the four test conditions. There was a trend of decreasing head acceleration from 15 to 30 degrees, and from driver side to passenger side positions. There was also a driver side to passenger side decrease in head acceleration, even though the passenger seat was further away from the effective center of rotation and had a relatively greater post impact velocity change. The test vehicle had seat back recliner adjusters only on the outboard sides of the front seats while the inboard seat backs had free moving hinges. The differential loading of compliant inboard, versus the stiffer outboard, sides apparently accounted for these paradoxical findings. Although there was a general pattern and similar timing in test subject responses, there were individual variations which were more evident during the relatively higher energy collisions.

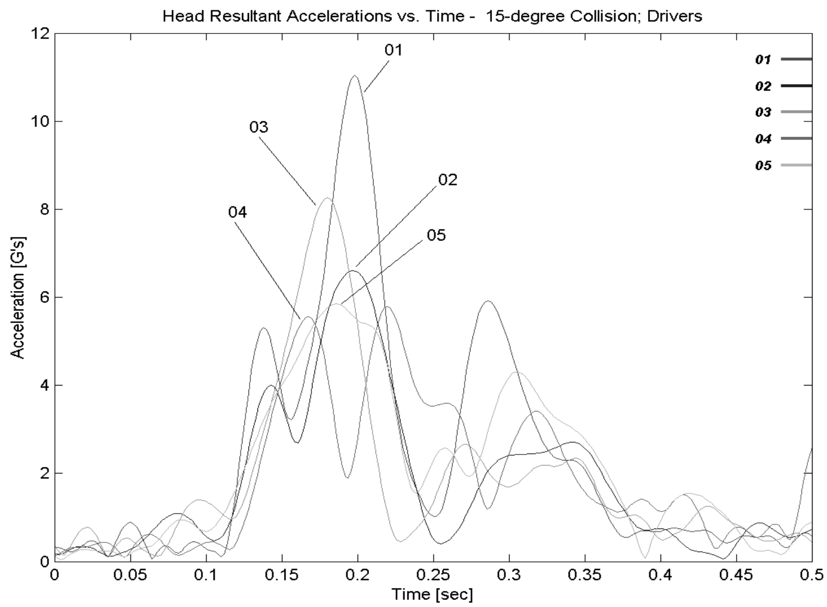
Head Resultant Accelerations vs. Time - 15-degree Collision; Drivers
Acceleration [G's]
Time [sec]
01
02
03
04
05

Fig. 13

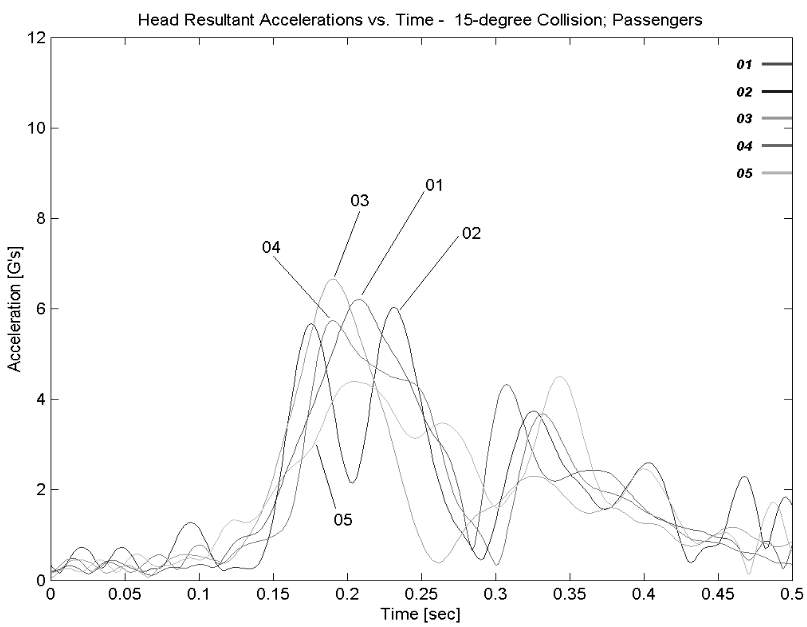
Head Resultant Accelerations vs. Time - 15-degree Collision; Passengers
Acceleration [G's]
Time [sec]
01
02
03
04
05

Fig. 14

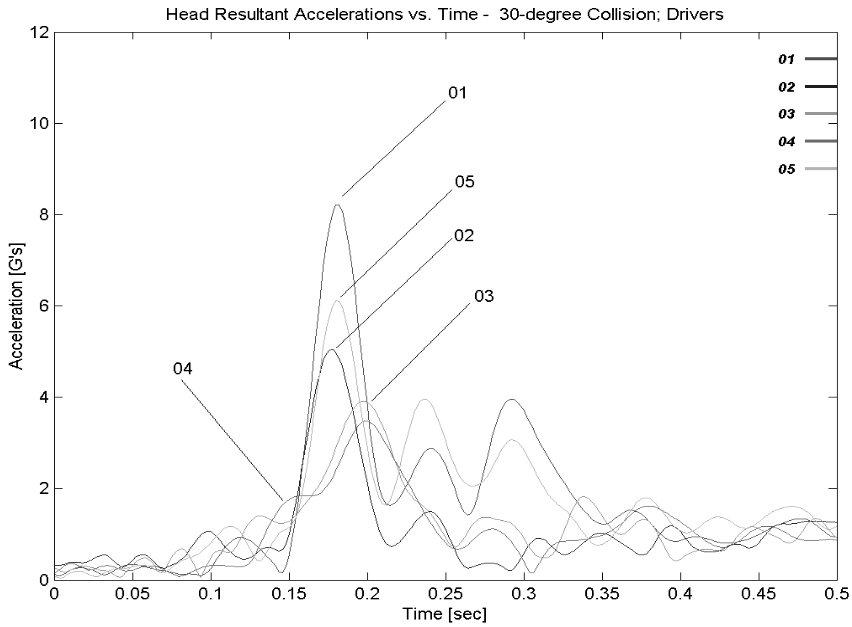

Fig. 15

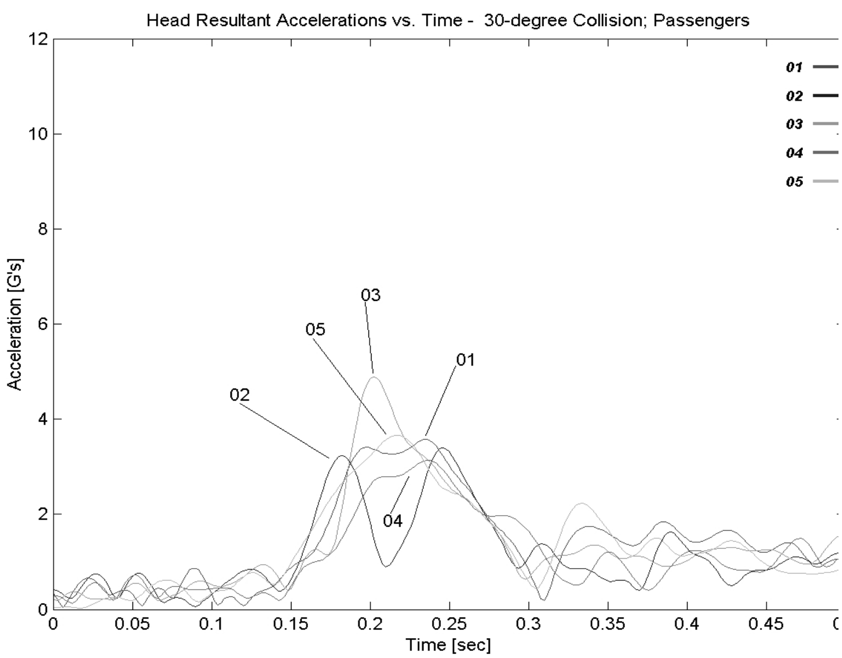

Fig. 16

Examples of such variation in resultant head accelerations are shown at Figs. 17 and 18 for the shortest (03) and tallest (04) subject respectively.

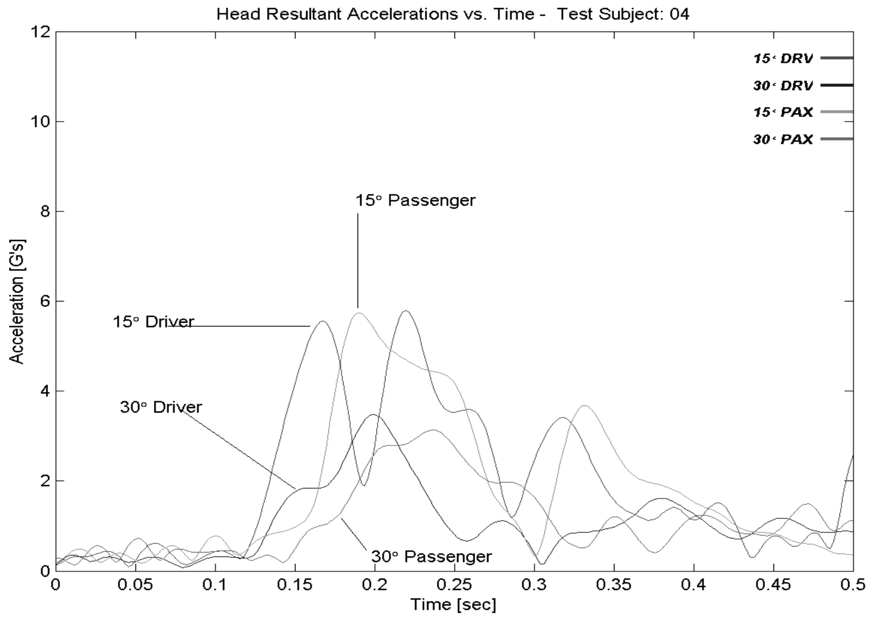

Fig. 17

The similarities in the patterns become more apparent when the response onset time differences in the crash pulse and onset of the velocity change in the various test conditions, is removed.

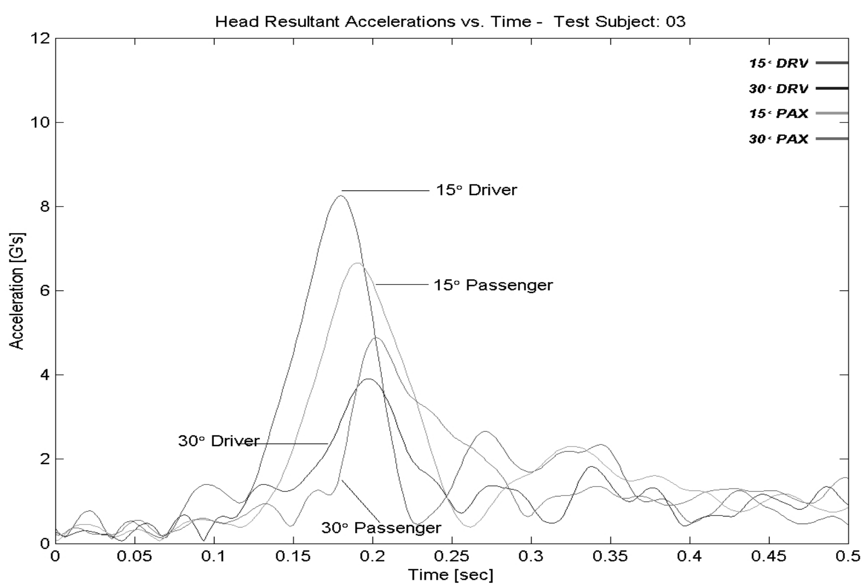

Fig. 18

Figs. 19 and 20 show the same data "time adjusted" to match the major peaks of the combined test graphs for the same subjects. When each pattern was compared to the HSF records, it appeared consistent with the peculiarities of each subject's interaction with the seat back and head restraint.

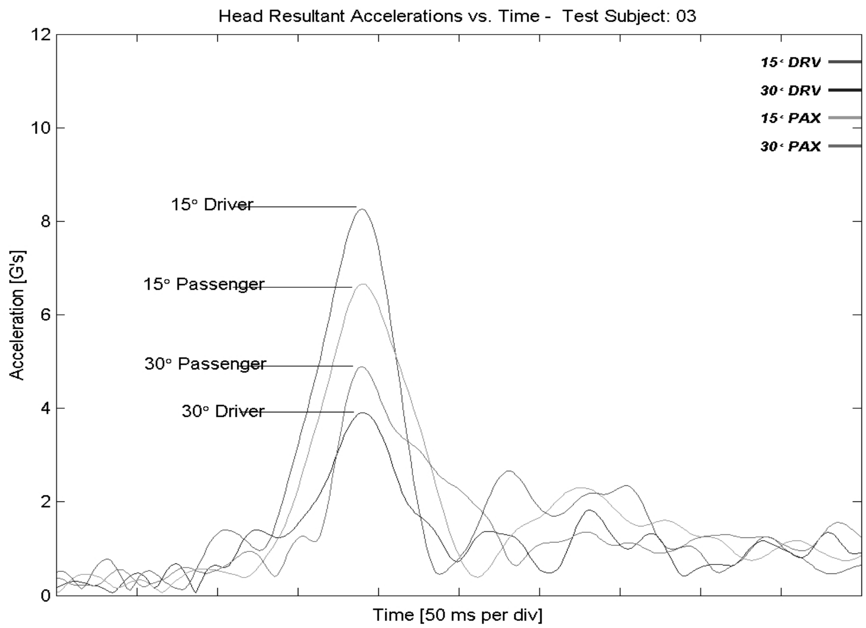
Head Resultant Accelerations vs. Time - Test Subject: 03
15° DRV
30° DRV
15° PAX
30° PAX
15° Driver
15° Passenger
30° Passenger
30° Driver
Acceleration [G's]
Time [50 ms per div]
0
2
4
6
8
10
12

Fig. 19

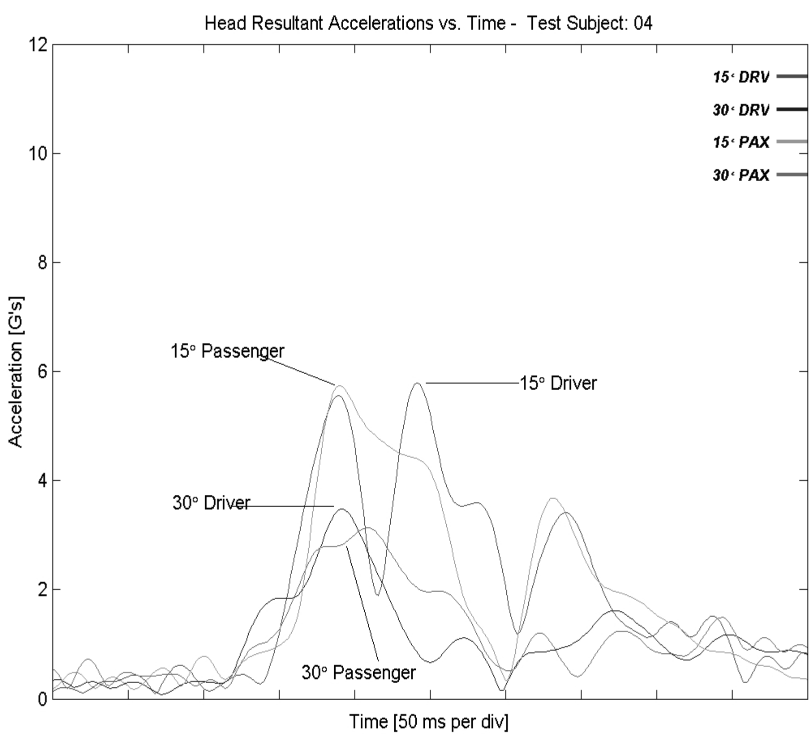
Head Resultant Accelerations vs. Time - Test Subject: 04
15° DRV
30° DRV
15° PAX
30° PAX
15° Passenger
15° Driver
30° Driver
30° Passenger
Acceleration [G's]
Time [50 ms per div]
0
2
4
6
8
10
12

Fig. 20

STATISTICAL EVALUATION - The results of the Matched-Pair Wilcoxon Signed-Ranks Test analysis of differences in head acceleration are given in Table 3.

Table 3 - Results of Statistical Comparisons of Peak Resultant Head Acceleration

Wilcoxon Test Results	Peak Head CG Acceleration (G)			Peak Bite-Block Acceleration (G)		
	W^+	W^-	Significance	W^+	W^-	Significance
Driver@15°> Driver@30°	14	1	$p < 0.10$	15	0	$p < 0.05$
Driver@15°> Pax@15°	15	0	$p < 0.05$	15	0	$p < 0.05$
Driver@30°> Pax@30°	13	2	$p < 0.10$	11	4	n.s.
Pax@15°> Pax@30°	15	0	$p < 0.05$	15	0	$p < 0.05$

Despite some driver head contacts during the 30 degree tests, the peak resultant accelerations of the head CG during the 15 degree tests were significantly higher for both seating positions. For both collision angles, however, the driver's position tended to show higher peak head acceleration than the passenger's. There was no statistical difference between the two seating positions at the 30 degree condition.

To remove the influence of the shape of the acceleration time-histories, they were integrated to produce an impact-related change in velocity for the head CG and bite-block. This integration produces a velocity change time-history, which peaks during the head over speed condition and decreases during the head restitution during phases 3 and 4.

The results of the Wilcoxon tests of the peak resultant velocity change differences are given in Table 4. The results of Wilcoxon tests of peak velocity change data indicate that the peak velocity changes for the head CG and the bite block were higher for both occupants in the 15 degree condition when compared to the 30 degree condition.

For the 15 degree condition, the differences by seating position were either weakly significant or not significant, depending on the velocity change estimate employed. For the 30 degree condition, the passenger's position showed a greater peak velocity change than that of the driver's position for the bite-block sensor; however the difference was not significant for the head CG velocity change. Thus, although the passengers in the 30 degree condition generally had lower peak head accelerations, they underwent a longer period of acceleration, which gave rise to a higher peak velocity change for their heads than that for the drivers.

Table 4 - Results of Statistical Comparisons of Resultant Head Velocity Change

Wilcoxon Test Results	**Peak Head CG ΔVelocity ($ft \cdot sec^{-1}$)**			**Peak Bite-Block ΔVelocity ($ft \cdot sec^{-1}$)**		
	W^+	**W^-**	Significance	**W^+**	**W^-**	Significance
Driver@15°> Driver@30°	15	0	$p < 0.05$	15	0	$p < 0.05$
Driver@15°> Pax@15°	10	0	$p < 0.10$	6.5	8.5	n.s.
Driver@30°< Pax@30°	4.5	10.5	n.s.	1	14	$p < 0.10$
Pax@15°> Pax@30°	15	0	$p < 0.05$	15	0	$p < 0.05$

VISUAL ANALYSIS - Fig. 21 shows an example of the similar kinematic response positions of all 5 test subjects during the 15 degree driver side tests at synchronized time points after the impact.

TEST RELATED CLINICAL FINDINGS - All test subjects were healthy and asymptomatic at the time of study. Several had prior LVRE test collision experience, but none reported residual effect, and all had normal physical examinations. Four subjects had normal cervical imaging studies, while the fifth had age-consistent changes of mild cervical spondylosis. None of these individuals reported acute or chronic cervical or lumbar symptoms. The initial six test runs of this series were accomplished in August and September 2000, while the remaining tests were completed from August to October 2001. There were no changes in either the constitution of the test panel or its medical status during this time. Although most tests met the desired seven days between exposures, three tests occurred within five or six days, and one morning test, in which a camera failed, was repeated on the same afternoon. To date none of the physician test subjects has described any delayed soft tissue discomfort symptoms and none has reported any complaints related to their participation in the test series. Test related symptoms reported by the test subjects are summarized in the Appendix.

Figs. 21 - 15 degree test: Comparison of Test Subject Kinematics (Side View).

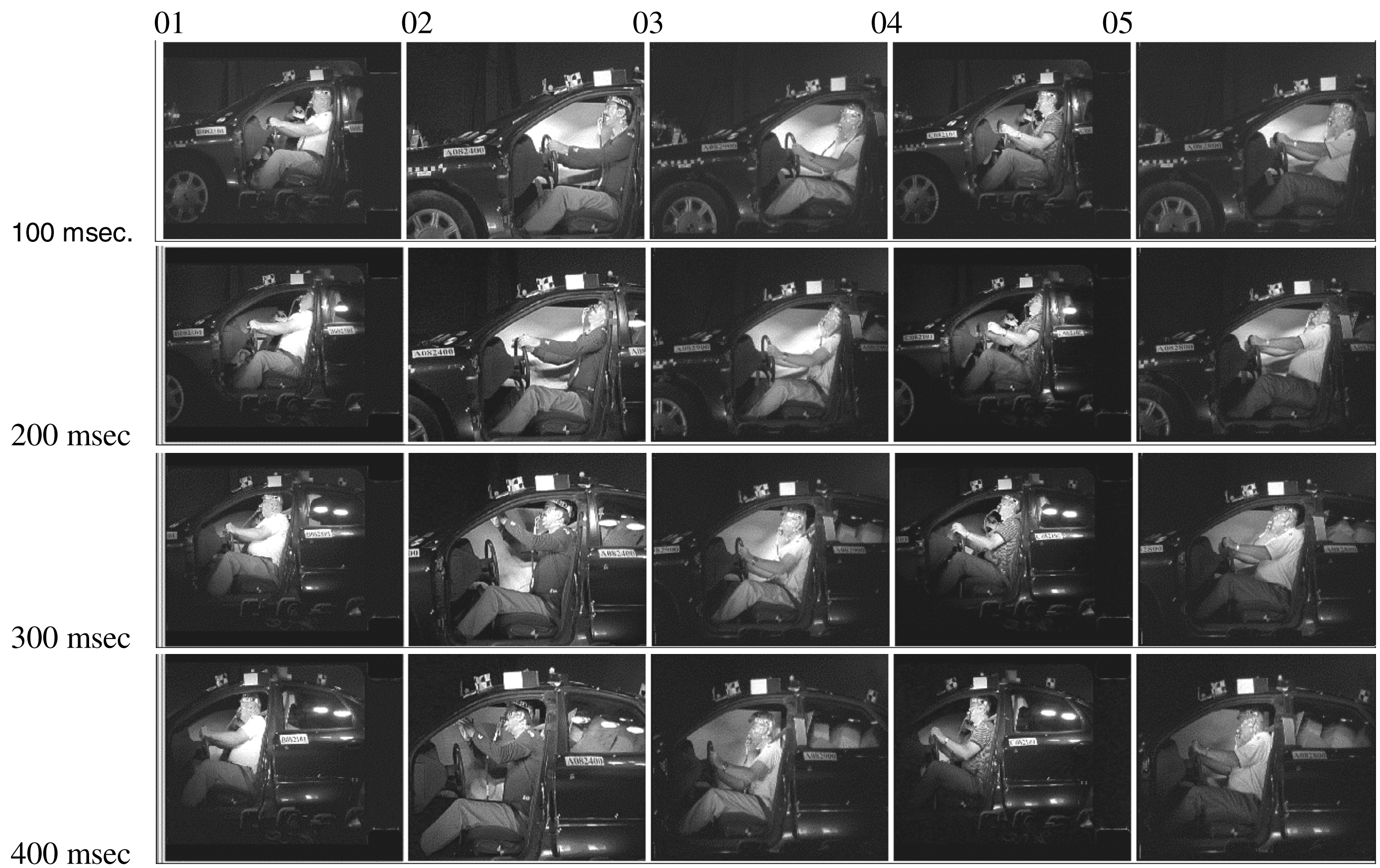

DISCUSSION

The vehicle dynamics of non-collinear LVRE collisions are highly dependent upon impact energy, angle of impact, line of action, suspension, tire sidewall characteristics, and tire to roadway coefficient of friction. The two variable collision conditions (line of action and angle of impact) in our test series demonstrated a yaw rotation about the left front wheel if the rear wheels lost traction. With no loss of traction, the body of the struck vehicle still yawed rightward, but less dramatically. In both cases the seat back acquired lateral motion with respect to the subject and altered his subsequent kinematic response. When the front and side camera HSF records of the test runs for each condition were viewed side by side and frame by frame, the similarity of each subject's kinematic response was marked. When, the acceleration profile for each individual was considered, and comparison made, subtle differences were apparent between the responses of each individual. The similar response of each individual to differing seat dynamic inputs present in this test series is consistent with dimensionally different, very complex masses of linked human parts interacting with the seat backs of the vehicle. Our data for each of the four test conditions indicate that the magnitude of upper body accelerations decreases as the lateral motion component of the collision increases. The lateral motion in turn depends upon the contributions made to it by impact energy, angle of impact, line of action, lateral tire traction, suspension system characteristics and rear tire sidewall compliance (flexibility). These factors will apply to other individuals and vehicles, but details will vary, as in this study. In addition, the passenger side tests in this study were associated with greater seat back deformation than were driver side tests. The Ford seat backs were evaluated with a spring scale and found to have consistently identical force-deflection characteristics for both positions, but the stiffness of the inboard side of both seats was approximately half that of the outboard side. It was concluded that seat back left-right stiffness differences were in part responsible for the variation in kinematic responses between the passenger and driver position.

CONCLUSIONS

This study was designed to elucidate, under defined and controlled conditions, the type of occupant kinematics that occur when a LVRE collision is non-collinear. Our results are a function of the physics of motion being applied to the human structure in a single, but typical, vehicle and seat. This study was not a statistically based investigation of injury likelihood, and does not predict expectations for a general population during various LVRE collision events. Rather, the study gathered data for just two sets of many possible configurations. Nevertheless, an underlying general kinematic response pattern was common to all five test subjects. While caution and well informed judgment must be used if this work is extrapolated to other types of non-collinear LVRE collisions, there is an underlying principle toward which our data point. The hypothesis that non-collinear LVRE collisions would have a greater potential for out-of-sagittal-plane head and neck kinematics than those seen during collinear LVRE collisions was supported by our results. There was, however, no indication of kinematic forcing of the subject's cervical spine into a position associated with increased injury likelihood. This study suggests that, for a given energy collision, the vehicle's velocity change (measured at the CG) and the related forces applied to the occupant diminish as impact angulation and rear tire side slip increase. The test vehicle's seat design played a significant role in the details of an individual's kinematic response. Based on our objective data, the exposure to nominal 8.0 kph (5 mph) increasingly non-collinear rear end collisions in this test series was correspondingly less likely to produce forced cervical motion approaching or beyond the anatomical/physiological limits of the neck. This conclusion is based on measured head accelerations and lack of induced cervical motion near or past the limits of physiological range of motion, as the impact angle and tire side slip increased. Conversely, as was shown in four of the 30 degree tests, as lateral vehicle motion increased, the potential for head contact with interior vehicle surfaces also increased for near side occupants. Further testing of these and other related conditions will be useful to further our understanding of occupant kinematics during angled low velocity impacts.

ACKNOWLEDGMENTS

This work was sponsored exclusively by our employers, Biodynamic Research Corporation and Injury Sciences LLC, using only their internal resources. Our special thanks go to the staff of the BRC Research Test Center, who patiently and with great innovation, made ideas and theory into working reality: Roy Meredith, John Kush, and Darrell Bay.

IN MEMORIAM

Richard P. Howard, M.D., 1934 - 2001, was our good friend, mentor, and colleague. He was a tireless seeker of the truth, and a truly remarkable and memorable gentleman. Without Dr. Howard's extraordinary drive, infectious enthusiasm, and generous support, our earlier LVRE collision work and this current effort simply would not exist.

REFERENCES

McConnell, W.E.; Howard, R.P.; Guzman, H.M.; Bomar, J.B.; Raddin, J.H., Jr.; Benedict, J.V.; Smith, H.L.; and Hatsell, C.P. (1993) Analysis of human test subject kinematic responses to low velocity rear end impacts. Presentation to Society of Automotive Engineers, Inc., 1993 SAE International Congress & Exposition, Detroit, MI, March 1993.

McConnell, W. E.; Howard, R. P.; Van Poppel, J.; Krause, R.; Guzman, H. M.; Bomar, J. B.; Raddin, J. H.; Benedict, J. V., and Hatsell, C. P. Human head and neck kinematics after low velocity rear-end impacts: understanding "whiplash". Proceedings of the 39th Stapp Car Crash Conference, San Diego, CA, November 8-10, 1995. Warrendale, PA, Society of Automotive Engineers. 1995; 215-238. SAE Paper #952724

Appendix A – Test and Clinical Symptoms Summary

Test #	Test Date	Struck Veh. Delta-V @CG Kph (mph)	Angle	Test Subject # - Position	Post Test Symptoms	Subsequent Symptoms & Notes
1	24Aug2000	9.0 (5.6)	15	02-Driver	@~5min post test – "twinge" in right superior trapezius, lasted < 1 minute	Day after – generalized cervical stiffness <24 hours
2	28Aug2000	9.0 (5.6)	15	05-Driver	Onset ~3-4 hours post test of right sternocleidomastoid muscle awareness	sternocleidomastoid muscle awareness gone next AM
3	29Aug2000	9.3 (5.8)	15	03-Driver	Noted mild sensation of non-painful chest compression during test	None
4	05Sep2000	6.4 (4.0)	30	04-Driver	Left parietal hair brushed left roof rail, no impact discomfort or swelling	None
5	08Sep2000	6.6 (4.1)	30	01-Driver	Mild upper left parietal scalp impact with left roof rail/B-pillar junction	No discomfort, no swelling, no sequellae
6	08Sep2000	6.6 (4.1)	30	05- Driver	Mild upper left parietal scalp impact with left roof rail/B-pillar junction	No discomfort, no swelling, no sequellae
7	21Aug2001	9.2 (5.7)	15	04-Driver	None noted	HSF Camera failed to run.
8	21Aug2001	9.3 (5.8)	15	01-Driver	None noted	None
9	21Aug2001	9.3 (5.8)	15	04-Driver	Fleeting discomfort left trapezius at neck base, lasted 1-2 seconds during impact	(Repeat exposure of test 7)
10	22Aug2001	6.6 (4.1)	30	03-Driver	Onset ~ 4 hours post test of inter-scapular "twinge" lasted into evening	No symptoms next day
11	29Aug2001	6.4 (4.0)	30	05-Pass	Onset ~ 2 hours post test of anterior neck strap muscle "awareness", lasted >1 hour	No recurrence, no sequellae
12	30Aug2001	6.4 (4.0)	30	04-Pass	None noted	None
13	30Aug2001	6.0 (3.7)	30	01-Pass	None noted	None
14	31Aug2001	6.3 (3.9)	30	03-Pass	None noted	None
15	04Sep2001	9.0 (5.6)	15	02-Pass	None noted	~12 hours post test - right sub-mandibular/hyoid soreness ~ 2 days
16	04Sep2001	9.0 (5.6)	15	01-Pass	Fleeting headache during test impact, lasted >1 sec	None
17	06Sep2001	9.2 (5.7)	15	04-Pass	None noted	None
18	06Sep2001	9.2 (5.7)	15	03-Pass	None noted	None
19	06Sep2001	9.2 (5.7)	15	05-Pass	None noted	None
20	14Sep2001	6.0 (3.7)	30	02-Pass	None noted	None
21	01Oct 2001	6.3 (3.9)	30	02-Driver	Mild upper left parietal scalp impact with left roof rail in front of B-pillar junction	No discomfort, no swelling, no sequellae